Task Refinement Learning for Improved Accuracy and Stability of Unsupervised Domain Adaptation

Yftah Ziser and **Roi Reichart**
Faculty of Industrial Engineering and Management, Technion, IIT
syftah@campus.technion.ac.il, roiri@ie.technion.ac.il

Abstract

Pivot Based Language Modeling (PBLM) (Ziser and Reichart, 2018a), combining LSTMs with pivot-based methods, has yielded significant progress in unsupervised domain adaptation. However, this approach is still challenged by the large pivot detection problem that should be solved, and by the inherent instability of LSTMs. In this paper we propose a *Task Refinement Learning (TRL)* approach, in order to solve these problems. Our algorithms iteratively train the PBLM model, gradually increasing the information exposed about each pivot. TRL-PBLM achieves state-of-the-art accuracy in six domain adaptation setups for sentiment classification. Moreover, it is much more stable than plain PBLM across model configurations, making the model much better fitted for practical use.[1]

1 Introduction

Domain adaptation (*DA*, (Daumé III, 2007; Ben-David et al., 2010)) is a fundamental challenge in NLP, as many language processing algorithms require costly labeled data that can be found in only a handful of domains. To solve this annotation bottleneck, DA aims to train algorithms with labeled data from one or more source domains so that they can be effectively applied in a variety of target domains. Indeed, DA algorithms have been developed for many NLP tasks and domains (e.g. (Jiang and Zhai, 2007; McClosky et al., 2010; Titov, 2011; Bollegala et al., 2011; Rush et al., 2012; Schnabel and Schütze, 2014)).

A number of approaches for DA have been proposed (§ 2). With the raise of Neural Networks (NNs), DA through Representation Learning (DReL) where a shared feature space for the source and the target domains is learned, has become prominent. Earlier DReL approaches (Blitzer et al., 2006, 2007) were based on a linear mapping of the original feature space to a new one, modeling the connections between pivot features – features that are frequent in the source and the target domains and are highly correlated with the task label in the source domain – and the complementary set of *non-pivot features*. This approach was later outperformed by autoencoder (AE) based methods (Glorot et al., 2011; Chen et al., 2012), which employ compress-based noise reduction to extract the shared feature space, but do not explicitly model the correspondence between the source and the target domains. Recently, methods that marry the complementary strengths of NNs and pivot-based ideas (Ziser and Reichart (2017, 2018a), denoted here with ZR17 and ZR18, respectively) established a new state-of-the-art.

Despite their strong empirical results, relying on NNs and on the distinction between pivot and non-pivot features, the models in ZR17 and ZR18 suffer from two limitations. These limitations stem from the fact that in order to create the shared feature space these models train NNs to predict the existence of pivot features in unlabeled data from the source and target domains (AEs in ZR17, LSTMs (Hochreiter and Schmidhuber, 1997) in ZR18). The first limitation is due to the large number of pivot features (several hundreds in each source/target domain pair in their experiments), which makes the classification task challenging and may harm the quality of the resulting cross-domain representations. As another limitation, NNs, and especially those that perform sequence tagging like *PBLM (Pivot Based Language Modeling, ZR18)*, are highly sensitive to model design and hyper-parameter selection decisions (Hutter et al., 2014; Reimers and Gurevych, 2017). Intuitively, if a DA approach is not robust across hyper-parameter configurations, it is more chal-

[1]Our code is publicly available at: `https://github.com/yftah89/TRL-PBLM`.

lenging to apply this approach to a variety of domain pairs. This is particularly worrisome in unsupervised domain adaptation (our focus setup, § 2), where no target domain labeled data is available, and hyper-parameter and configuration tuning is performed on source domain labeled data only.

In this paper we propose to solve both problems by applying a novel *Task Refinement Learning (TRL) approach* to the state-of-the-art PBLM representation learning model (§ 3). In our TRL-PBLM model the PBLM is trained in multiple stages. At the first stage the model should predict only the core relevant information each pivot holds with respect to the domain adaptation task. We do this by clustering the pivots with respect to the information they convey about the domain adaptation task and asking the model to predict the clusters rather than the pivots themselves. Then, at subsequent stages, the model should predict an increasingly larger subset of the pivots, while for those pivots that have not yet been exposed it is only their cluster that should be predicted. The pivots exposed in each iteration are defined based on measures of the complexity of the prediction task associated with each pivot and the importance of the pivot for the domain adaptation task.

At each stage the PBLM is trained till convergence and its learned parameters then initialize the PBLM that is trained at the next stage. This transfer of information between stages is possible because the complexity of the prediction task with respect to each pivot (predicting the cluster or the pivot itself) can only increase between subsequent stages. Since PBLM is non-convex and hence sensitive to its initialization, each training stage of PBLM exploits the outcome of the learning task of its predecessor. Only at the last stage PBLM should predict the full set of pivot features, as in the standard PBLM training of ZR18.

We hypothesize that TRL is a suitable solution for both aforementioned problems. For the large number of classes, TRL-PBLM starts from a small classification problem at the first stage and the number of classes gradually increases in subsequent stages, reaching the maximum only at the last stage. Moreover, the model should gradually predict increasingly more complex pivots that provide more fine grained information about the task. This way it should predict the existence of complex pivots only after it has learned about simpler ones. For configuration instability, we hypothesize that the gradual training of the model should result in a smoother convergence and a smaller impact of arbitrary design choices.

Our approach is inspired by curriculum learning (CL (Elman, 1993; Bengio et al., 2009)), a learning paradigm that advocates the presentation of training examples to a learning algorithm in an organized manner, so that more complex concepts are learned after simpler ones. Indeed, CL methods have been designed for many NLP tasks (e.g. (Turian et al., 2010; Spitkovsky et al., 2010; Zou et al., 2013; Shi et al., 2015; Sachan and Xing, 2016; Wieting et al., 2016)) and for other machine learning application areas such as computer vision (e.g. (Pentina et al., 2015; Oh et al., 2015; Gong et al., 2016; Zhang et al., 2017)). However, while in CL the prediction task is fixed but the trained algorithm is exposed to increasingly more complex training examples in subsequent stages, in TRL the algorithm is trained to solve increasingly more complex tasks in subsequent stages, but the training data is kept fixed across the stages.

We implemented the experimental setup of ZR18 for sentiment classification, considering all their 5 domains for a total 6 domain pairs (§ 4).[2] Our TRL-PBLM-CNN model is identical to the state-of-the-art PBLM-CNN of ZR18, except that PBLM is trained with one of our TRL methods. Our best performing model outperforms the original PBLM-CNN by 2.1% on average across the six setups (80.9% vs. 78.8%). For two domain pairs, the improvement is as high as 5.2% (80.2% vs. 75%) and 3.6% (86.1% vs. 82.5%).

Moreover, TRL-PBLM-CNN is more robust than plain PBLM-CNN, consistently achieving a higher maximum, minimum and average results as well as a lower standard deviation across the 30 configurations we considered for each model. We consider this a major result since, as noted above, stability is crucial for the real-world applicability of an unsupervised domain adaptation algorithm, since the selection of model configuration in this setup does not involve target domain labeled data and is hence inherently noisy and risky.

2 Background and Previous Work

Domain adaptation is a long standing NLP challenge (Roark and Bacchiani, 2003; Chelba and

[2]Since TRL-PBLM requires multiple PBLM training stages, it was computationally demanding to experiment with all the 20 domain pairs of ZR18. See § 4 for more details.

Acero, 2004; Daumé III and Marcu, 2006). Major approaches to DA include: instance re-weighting (Huang et al., 2007; Mansour et al., 2009), sub-sampling from both domains (Chen et al., 2011) and DA through Representation Learning (DReL) where a joint source and target feature representation is learned. DReL has shown to be the state-of-the-art for unsupervised DA (Ziser and Reichart, 2017, 2018a,b), and is the approach we pursue.

Unsupervised Domain Adaptation In this work we focus on unsupervised DA. In this setup we have access to unlabeled data from the source and the target domains, but labeled data is available in the source domain only. We believe this is the most realistic setup if one likes to extend the reach of NLP to a large number of domains.

The pipeline of unsupervised DA with representation learning typically consists of two steps: representation learning and classification. In the first step, a representation model is trained on the unlabeled data from the source and target domains. In the second step, a classifier for the supervised task is trained on the source domain labeled data and is then applied to the target domain. Every example that is fed to the task classifier is first represented by the representation model of the first step. This is the pipeline we follow in our models.

In unsupervised DA the representation model and the task classifier can also be trained jointly. In § 4 we compare our models to such an end-to-end model (MSDA-DAN (Ganin et al., 2016)).

Domain Adaptation with Representation Learning (DReL) A seminal DReL model, from which we start our survey, is Structural Correspondence Learning (SCL) (Blitzer et al., 2006, 2007) that introduced the idea of pivot-based DReL. The main idea is to identify in the shared feature space of the source and the target domains the set of pivot features that can serve as a bridge between the domains. Formally these pivot features are defined to be: (a) frequent in the unlabeled data from both domains; and (b) highly correlated with the task label in the source domain labeled data. The remaining features are referred to as non-pivot features.

In SCL, the division of the original feature set into the pivot and non-pivot subsets is utilized in order to learn a *linear* mapping from the original feature space of both domains into a shared, low-dimensional, real-valued feature space. Since SCL was presented, pivot-based DReL has been researched extensively (e.g. (Pan et al., 2010; Gouws et al., 2012; Bollegala et al., 2015; Yu and Jiang, 2016; Ziser and Reichart, 2017, 2018a)).

In contrast to SCL that learns a linear transforamtion between pivot and non-pivot features, the next line of work aimed to learn representations with non-linear models, without making the distinction between pivot and non-pivot features. The basic idea of these models is training an autoencoder (AE) on the unlabeled data from both the source and the target domains, reasoning that the hidden representation of such a model should be less noisy and hence robust to domain changes.

Examples of AE variants in recent DReL literature include Stacked Denoising Autoencoders (SDA, (Vincent et al., 2008; Glorot et al., 2011), the more efficient and salable marginalized SDA (MSDA, (Chen et al., 2012)), and MSDA variants (e.g. (Yang and Eisenstein, 2014; Clinchant et al., 2016)). Models based on variational AEs (Kingma and Welling, 2014; Rezende et al., 2014) have also been applied in DA (e.g. variational fair autoencoder (Louizos et al., 2016)), but they were outperformed by MSDA in Ziser and Reichart (2018a).

Ziser and Reichart (2017) combined AEs with pivot-based DA. Their models (AE-SCL and AE-SCL-SR) are based on a three layer feed-forward network where the non-pivot features are fed to the input layer, encoded into a hidden representation and this hidden representation is then decoded into the pivot features of the input example. AE-SCL-SR utilizes word embeddings to exploit the similarities between pivot-based features, outperforming AE-SCL, and many other DReL models.

A major limitation of the ZR17 models is that they do not exploit the structure of their input examples, which can harm document level tasks. We next describe an alternative approach.

Pivot Based Language Modeling (PBLM) PBLM is a variant of an LSTM-based language model (LSTM-LM). However, while an LSTM-LM predicts at each point the most likely next input word, PBLM predicts the next input unigram or bigram if one of these is a pivot (if both are, it predicts the bigram) and NONE otherwise.[3] In the unsupervised DA pipeline PBLM is trained with the source and target domain unlabeled data.

Consider the example in Figure 1a (imported

[3]In § 4 we describe the automatic pivot selection method which is solely based on the labeled and unlabeled data.

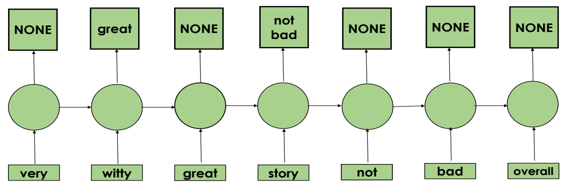

(a)

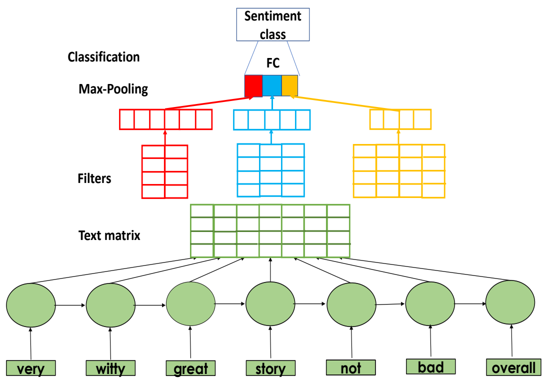

(b)

Figure 1: The PBLM model (figures imported from ZR18). (a) The PBLM representation learning model. (b) PBLM-CNN where PBLM representations feed a CNN task classifier.

from ZR18) for adaptation of a sentiment classifier between book reviews and reviews of kitchen appliances. In this example PBLM learns the connection between the book related (and hence non-pivot) adjective *witty*, and *great* - a common positive adjective in both domains, and hence a pivot. PBLM is designed to feed structure-aware task classifiers. Particularly, in the PBLM-CNN architecture that we consider here (Figure 1b),[4] the PBLM's softmax layer (that computes the probabilities of each pivot to be the next unigram/bigram) is cut and a matrix whose columns are the PBLM's h_t vectors is fed to the CNN.

ZR18 demonstrated the superiority of PBLM-CNN over previous approaches to DReL, establishing the importance of structure-aware representation learning for review document modeling. We hence develop our TRL methods for PBLM.

3 Task Refinement Learning for PBLM

We apply TRL only to the representation learning stage of the unsupervised domain adaptation pipeline. We first describe the general TRL scheme, and then list specific implementations.

3.1 A General TRL Scheme

As noted in § 2, PBLM is similar to an LSTM language model, but instead of predicting the next word at each position, it predicts the next unigram or bigram if these are pivots and a special NONE symbol otherwise. Our TRL scheme gradually exposes pivots to PBLM (Algorithm 1).

We start by dividing the pivot features into two subsets: *PosPiv* is the set of pivot features that are more frequent in source domain training documents with positive labels than in source domain documents with negative labels; *NegPiv* is similarly defined, but these pivots are more frequent in source domain training documents with a negative label. In the first stage, PBLM is trained on the unlabeled data from the source and the target domains till convergence, just as in ZR18. The only difference is that in cases where the next unigram or bigram is a pivot, instead of predicting the actual pivot identity, PBLM should predict *PosPiv* or *NegPiv* according to the pivot's class. That is, the representation learned by the first PBLM model is only sensitive to whether a pivot is positive or negative and not to the actual pivot identity. Following the definition of pivot features (§ 2), the positive/negative distinction is fundamental, and is hence considered at the first TRL stage.

```
Data: $U_s$: unlabeled source domain data; $U_t$:
        unlabeled target domain data.
Input: $K$: number of TRL iterations;
  SortPivots: a sorted array of pivots; NegPiv:
  the list of negative pivots; PosPiv: the list of
  positive pivots.
$\theta^0$ = rand();
$\theta^1$ = PBLMTrain ($\theta^0$, NegPiv, PosPiv, $U_s$,
  $U_t$);
i = 1;
while $i \leq K$ do
    $\theta$ = update-PBLM-params ($\theta^i$, NegPiv,
      PosPiv, SortPivots, i);
    $\theta^{i+1}$ = PBLMTrain ($\theta$, NegPiv, PosPiv,
      SortPivots, i, $U_s$, $U_t$);
    i = i + 1;
end
return $\theta^i$;
```

Algorithm 1: TRL for PBLM.

After this initial step is completed our TRL algorithm continues for a predefined number of iter-

[4]ZR18 also considered a PBLM-LSTM architecture where the PBLM representations feed an LSTM classifier. We focus on PBLM-CNN which demonstrated superior performance in 13 of 20 of their experimental setups.

ations (denoted with K in Algorithm 1). The algorithm receives as input a sorted array of pivot features such that pivots at the beginning of the array (lower indices) should be exposed first. At each iteration the PBLM is exposed to additional $\#_P/K$ pivots, where $\#_P$ is the total number of pivot features. That is, at the first iteration the first $\#_P/K$ pivots are exposed, at the second iteration the next $\#_P/K$ are also exposed and so on till the last (K-th) iteration in which all pivots are exposed. Since new features are exposed in each iteration, the label space of PBLM changes. For example, before the first iteration the label space consists of three labels: NONE, PosPiv and NegPiv, while in the first iteration the label space consists of NONE, PosPiv (for all positive pivots that are not exposed in this iteration), NegPiv (for all negative pivots that are not exposed in this iteration) and the first (top ranked) $\#_P/K$ pivots in the sorted pivot array, for a total of $\#_P/K$ + 3 labels.

At each iteration the algorithm first updates the PBLM parameters (up-PBLM-params method of Algorithm 1). In this step a new PBLM model is initialized such that all its parameters except for those of the softmax prediction matrix are initialized to the parameters to which PBLM converged in the last time it was trained. The softmax matrix grows so that it can predict $i \cdot \#_P/K + 3$ labels, instead of $(i - 1) \cdot \#_P/K + 3$ labels as in the previous PBLM training (i is the iteration number). To do that, the weights for the NONE, PosPiv and NegPiv classes as well as for the pivots that were exposed before the current iteration are initialized to the output of the previous PBLM training, while the weights of the newly exposed pivots are initialized to the weights learned for PosPiv (for those newly exposed pivots that were assigned the PosPiv label in the previous run) or for NegPiv (for those newly exposed pivots that were assigned the NegPiv label in the previous run). After the parameters are initialized, PBLM is trained again and the process proceeds iteratively till the last iteration where all the pivots are exposed. The weights of the last iteration will be used when PBLM is employed at the classification stage of the unsupervised DA pipeline (§ 2).

Example To make the above explanation more concrete, we consider an example in which we have four pivots: *good, bad, great* and *worst*, so that *good* and *great* belong to PosPiv while *bad* and *worst* belong to NegPiv. We set K, the number of iterations, to 2, which means that the number of features exposed in each iteration is $\#_P/K = 4/2 = 2$. Finally, we assume that our pivot ranking method ranks the pivots in the order in which they were presented above.

PBLM is first trained so that at each position if the next word is *good* or *great* it should predict PosPiv, if it is *bad* or *worst* it should predict NegPiv and otherwise it should predict NONE. Then the pivot exposure iterations begin. At the first iteration the pivots *good* and *bad* are exposed. The parameters learned in the previous run of PBLM (with the PosPiv, NegPiv and NONE predictions) are used as an initialization of the PBLM parameters, except that the softmax matrix should now allow five classes: PosPiv (for occurrences of *great*, that has not been exposed yet), NegPiv (for occurrences of *worst*), *good*, *bad* and NONE. Hence, in the softmax matrix of the new PBLM the parameters for PosPiv, and also for good, will be the parameters learned in the previous iteration for PosPiv. Likewise, the parameters for NegPiv, and also for bad, will be the parameters learned in the previous iteration for NegPiv, and the parameters for NONE are those previously learned for NONE.

At the second iteration, the last two pivots, *great* and *worst*, are also exposed, and PBLM now has the following 5 classes: *good*, *bad*, *great*, *worst* and NONE. Parameter initialization is done in a similar manner to the first iteration, where the softmax parameters for *great* and *worst* are initialized to the parameters of PosPiv and NegPiv of the previous PBLM, respectively. Finally, this last PBLM is trained to yield the model that will be used in the unsupervised DA setup.

We next describe our three methods for the order in which pivots are exposed in TRL training.

3.2 Pivot Exposure in TRL

Our goal is to order the pivots so that highly ranked pivots convey more information about the domain adaptation task and are easier to predict by PBLM. We consider three pivot ranking methods.

The **Ranking by MI (RMI)** method ranks the pivots according to their mutual information (MI) with the task label in the source domain training data. The reasoning is that pivots that are more strongly associated with the task label provide a stronger task signal to the representation learning model and should hence be learned earlier in the process. A downside of this method is that it does not consider any target domain information.

Another alternative is the **Ranking by Frequency (RF)** method that ranks pivots according to the number of times they appear in the unlabeled data of both the source and target domains (combined). The reasoning here is that the representation learning model should have more statistics about the frequent pivots, which makes their prediction easier. Moreover, the frequent pivots presumably provide a more prominent signal about the desired representation and should hence be learned prior to less frequent pivots, whose signal is more nuanced. One obvious advantage of this method is that it considers both the source and the target domain. However, in cases where a pivot is very frequent in one domain and substantially less frequent in the other, RF would consider this pivot frequent, even though it does not provide too much information about one of the domains.

To overcome this limitation of RF, we also consider a third pivot ranking method: **Ranking by Similar Frequencies (RSF)**. In this method we compute two quantities for each pivot: $f_{p-source} = \frac{\#_{ps}}{\#_{sd}}$ and $f_{p-target} = \frac{\#_{pt}}{\#_{td}}$, where $\#_{ps}$ is the number of times the pivot p appears in the source domain unlabeled data, $\#_{sd}$ is the number of documents in the source domain labeled data, and $\#_{pt}$ and $\#_{td}$ are defined similarly for the target domain unlabeled data. We then compute the similar frequency score of each pivot p to be: $freqScore(p) = \frac{min(f_{p-source}, f_{p-target})}{max(f_{p-source}, f_{p-target})}$, and rank the pivots in a descending order of $freqScore$ scores. This way, pivots with more similar frequencies in the unlabeled data of both domains are ranked higher and will be exposed earlier to the PBLM algorithm.

4 Experiments

We implemented the setup of ZR18, including datasets, baselines, and hyperparameter details.

Task and Domains Following ZR18, and a large body of DA work, we experiment with the task of binary cross-domain sentiment classification with the product review domains of Blitzer et al. (2007) – Books (B), DVDs (D), Electronic items (E) and Kitchen appliances (K). We also consider the airline review domain that was presented by ZR18, who demonstrated that adaptation from the Blitzer product domains to this domain, and vice versa, is more challenging than adaptation between the Blitzer product domains.

For each of the domains we consider 2000 labeled reviews, 1000 positive and 1000 negative, and unlabeled reviews: 6000 (B), 34741 (D), 13153 (E), 16785 (K) and 39396 (A). Since PBLM is computationally demanding, and employing TRL to PBLM requires multiple PBLM training processes, we pick 6 setups from the 20 of ZR18. We include each of the domains considered in ZR18 at least once. Our setups are: B-D, B-K, E-D, K-B, A-B and K-A.

Models and Baselines Our main baseline is the PBLM-CNN sentiment classifier – the superior model of ZR18 (§ 2) – to which we refer as *NoTRL*. Our TRL algorithm aims to improve the PBLM (representation learning) step of the PBLM-CNN model. We consider the three TRL methods of § 3.2: *Ranking by MI (RMI)*, *Ranking by Frequency (RF)*, and *Ranking by Similar Frequencies (RSF)*, each protocol is implemented with either $K = 4$ or $K = 2$ iterations, in addition to the initial step where the pivots are split into the positive and negative classes. The model names are hence: *RMI2, RMI4, RF2, RF4, RSF2 and RSF4*. To evaluate the relative importance of the initial pivot split to positive, negative and non-pivot classes compared to the pivot exposure methods, we also add the *BasicTRL* model in which the basic three class PBLM training is followed by a single iteration where all the pivots are exposed.

To put our results in the context of previous leading models we further compare to the prominent baselines of ZR18: *AE-SCL-SR*; *SCL* with pivot features selected using the mutual information criterion *(SCL-MI, (Blitzer et al., 2007))*; MSDA and *MSDA-DAN* (Ganin et al., 2016) which employs a domain adversarial network (DAN) with MSDA vectors as input. Finally, we compare to a *NoDA* setup where the sentiment classifier is trained in the source domain and applied to the target domain without adaptation. For this case we consider a logistic regression classifier that was demonstrated in ZR18 to outperform LSTM and CNN classifiers. This is also the classifier employed with AE-SCL-SR and SCL-MI. [5]

Features and Pivots The input features of all models are word unigrams and bigrams. The division of the feature set into pivots and non-pivots is based on Blitzer et al. (2007) and (Ziser and Re-

[5]The URLs of the datasets and the code we used, are provided in the appendix.

ichart, 2017, 2018a): Pivot features appear at least 10 times in the unlabeled data of both the source and the target domains, and among those features are the ones with the highest mutual information with the task (sentiment) label in the source domain labeled data. For non-pivot features we consider unigrams and bigrams that appear at least 10 times in the unlabeled data of at least one domain.

Cross-Validation and Hyperparameter Tuning We employ a 5-fold cross-validation protocol as in ZR18. In all five folds 1600 source domain examples are randomly selected for training data and 400 for development, such that both the training and the development sets have the same number of positive and negative reviews. For each model we report the averaged performance across these 5 folds. For previous models, we follow the tuning process of ZR18. The tuning of PBLM and of our TRL methods is described in the Appendix.

5 Results

Overall Performance Our first result is presented in Table 1. On average across the test sets, all TRL-PBLM methods improve over the original PBLM (NoTRL) with the best performing method, RF2, improving by as much as 2.1% on average (80.9 vs. 78.8). In all 6 setups one of the TRL-PBLM methods performs best. In two setups RF2 improves over NoTRL by more than 3.5%: 80.2 vs 75 (E-D) and 86.1 vs 82.5 (B-K) (error reduction of 20.8% and 20.6%, respectively). In two other setups RF2 improves by 1.7-2%: K-B (76.2 vs. 74.2), and A-B (72.3 vs. 70.6). In the remaining two setups a TRL method improves, although by less than 0.5%. The 80.9% averaged accuracy of RF2 compares favorably also with the 74.4% of AE-SCL-SR, the strongest baseline from ZR18.

Test Set Stability Our second result is presented in Table 2. The table presents the minimum (min), maximum (max), average (avg) and standard deviation (std) of the test set scores of the 30 hyper-parameter configurations we consider for each model. The table compares these numbers for RF2, our best performing TRL-PBLM method, BasicTRL, that exposes all the pivots in the first iteration after PBLM is trained with the positive, negative and non-pivot classes, and for NoTRL.

The table clearly demonstrates that RF2 and BasicTRL consistently achieve higher avg, max and min results, as well as a lower std, compared to adaptation with NoTRL. This means that models learned by TRL based methods are much more robust to the selection of the hyper-parameter configuration. Moreover, even the min values of RF2 consistently outperform the NoDA model (where a classifier is trained on the source domain and applied to the target domain without domain adaptation; bottom line of Table 1) and the min values of BasicTRL outperform NoDA in 5 of 6 setups (average difference of 3.9% for RF2 and for 3.5% for BasicTRL). In contrast, the min value of NoTRL is outperformed by NoDA in 5 of 6 cases (with an averaged gap of 2.8%).

Model Selection Stability Additional comparison between Table 2 and Table 1 further reveals that model selection by development data has a more negative impact on NoTRL, compared to RF2 and BasicTRL. Particularly, for NoTRL there are only two cases where the model that performs best on the test set (max column of Table 2) was selected by the development data (the numbers reported in Table 1): B-D (84.2%) and K-A (86.1%). Moreover, the averaged difference between the best test set model and the one selected by the development data for NoTRL is 1.3%, and in one setup (E-D) the difference is as high as 4.3%. For RF2, in contrast, there are four cases where the best performing test set model is selected by the development data (E-D, K-B, A-B and K-A), and the averaged gap between the selected model and the best test set model is only 0.1%. For BasicTRL the corresponding numbers are two setups and an averaged difference of 0.6%. These improved stability patterns are observed also with the other TRL methods we experiment with. We do not provide additional numbers in order to keep our presentation concise.

Finally, we note that BasicTRL preforms well, despite being simpler than the other TRL models. For example, in three of the six Table 1 setups BasicTRL is the second best model and in one setup it is the best model. Table 2 also reflects similar performance for RF2 and BasicTRL. Likewise, for all pivot exposure methods 2 iterations are somewhat better than 4. In future work we intend to explore additional pivot exposure strategies.

Ablation Analysis We finally consider a possible explanation to the success of TRL. Recall that the goal of PBLM is to encode the input text in a way that preserves the information in the pivots.

	B-D	**B-K**	**E-D**	**K-B**	**A-B**	**K-A**	**Average**
PBLM+TRL Methods							
RF2	84.1	**86.1**	**80.2**	**76.2**	**72.3**	86.1	**80.9**
RF4	83.4	85	79.2	73.7	71	**86.5**	79.8
RSF2	84	85.1	79.1	74	71.3	85.9	79.9
RSF4	83.4	85.3	78	74.1	69.7	86	79.4
RMI2	83.5	85.4	79.2	74.1	69.6	86.2	79.7
RMI4	83.5	84.9	78.1	72.8	69.4	86.1	79.1
BasicTRL	**84.4**	85.9	78.2	74.6	70.8	86.4	80.1
Plain PBLM (ZR18)							
NoTRL	84.2	82.5	75	74.2	70.6	86.1	78.8
Other Baselines							
AE-SCL-SR	81.1	80.1	74.5	73	60.5	76.9	74.4
MSDA	78.3	78.8	71	70	58.5	76.8	72.2
MSDA-DAN	79.7	75.4	73.1	71.2	59.5	76.6	72.6
SCL	78.8	77.2	70.4	69.3	61.7	72.3	71.6
NoDA	76	74	69.1	67.6	57.5	69.6	67

Table 1: Sentiment accuracy when hyper-parameters are tuned with development data.

B-D				
	avg	**max**	**min**	**std**
RF2	82.2	84.5	79	1.20
BasicTRL	82.6	84.6	80.5	0.94
NoTRL	78.3	84.2	70.2	3.70
B-K				
	avg	**max**	**min**	**std**
RF2	82.7	86.3	78.9	1.96
BasicTRL	83.3	85.9	80.5	1.46
NoTRL	78.6	84.1	71.3	3.30
E-D				
	avg	**max**	**min**	**std**
RF2	75.8	80.2	70	2.40
BasicTRL	75.4	79.8	69.6	2.50
NoTRL	71.7	79.3	65.9	3.40
K-B				
	avg	**max**	**min**	**std**
RF2	72.1	76.2	68.6	1.70
BasicTRL	72	74.9	66.1	2.24
NoTRL	68.8	74.4	62.8	3.78
A-B				
	avg	**max**	**min**	**std**
RF2	65.6	72.3	61.6	2.20
BasicTRL	65.7	72.3	61.3	2.10
NoTRL	64.8	71.6	60.9	2.70
K-A				
	avg	**max**	**min**	**std**
RF2	83.6	86.1	78	2
BasicTRL	84.3	86.4	76.9	1.90
NoTRL	76.1	86.1	66.2	6.80

Table 2: Statistics of the test set accuracy distribution achieved by the PBLM-CNN sentiment classifier, when adapted between domains with RF2, BasicTRL, and NoTRL (the first two are TRL-based methods). The statistics are computed across 30 model configurations.

	B-D	**B-K**	**E-D**	**K-B**	**A-B**	**K-A**
RF2	98.4	98.9	99.3	98.6	99.5	99.2
B-TRL	97.9	99.0	99.2	95.5	99.0	98.4
NoTRL	78.2	81.7	81.2	78.3	72.5	76.1

Table 3: Ablation analysis. B-TRL is BasicTRL.

This encoding (the hidden vectors of the LSTM) is then fed to the task classifier. We can hence expect that in a high quality PBLM model the representation of pivots (their vectors in the softmax output matrix of the model) from the PosPiv class (§3.1) will be similar to each other, and the representation of pivots from the NegPiv class will be similar to each other, but that members of the two classes will have distinct representations. This way we are promised that the input text encoding preserves an important bit in the pivots' semantics: their correspondence to one of the sentiment labels.

For RF2, BasicTRL and NoTRL we hence perform the following analysis, focusing on the models with 500 pivots. After the model converges we compute for each of the 500 pivots its 10 nearest neighbor and compute the percentage of these neighbors that belong to the same class, PosPiv or NegPiv, as the pivot. In Table 3 we report for each model the average over the 3000 scores we get from the six model configurations we trained with 500 pivots (see the appendix for the details of the configurations). The table clearly demonstrates that the pivot representations learned by RF2 and BasicTRL clustered much better to the PosPiv and

NoTRL		BasicTRL		RF2	
pivot	**sentiment**	**pivot**	**sentiment**	**pivot**	**sentiment**
would_recommend	positive	would_highly	positive	would_recommend	positive
love	positive	would_recommend	positive	would_highly	positive
recommend_them	positive	happy	positive	recommend_them	positive
remember	positive	recommend	positive	happy	positive
not_recommend	negative	recommend_them	positive	love	positive
happy	positive	enjoyed	positive	I_highly	positive
thought	negative	only_complaint	positive	remember	positive
would_not	negative	appreciate	positive	recommend	positive
not_buy	negative	I_highly	positive	never_have	positive
I_highly	positive	saves	positive	appreciate	positive

Table 4: Top 10 nearest neighbors (ranked from the closest neighbor downward) of the pivot "highly recommended" according to three models: NoTRL (plain PBLM), BasicTRL and RF2. TRL training results in all members of the neighbor list of a pivot being of the same sentiment class as the pivot itself.

NegPiv clusters compared to the pivot representations in NoTRL. This means that the encoding of the input with respect to the pivots preserves the sentiment class information much better in these TRL models than in the NoTRL model.

To illustrate this effect, we present here a qualitative example of the nearest neighbor list of a pivot according to three models (Table 4). The domain adaptation setup of the example is K-A and the pivot we selected for this example is *highly recommended* which falls into the PosPiv class (i.e. it appears many more times in positive source domain reviews than in negative ones). The table demonstrates that for the NoTRL model there are several NegPiv pivots in the nearest neighbor list of *highly recommended* – e.g. *not recommend* and *not buy*. In contrast, the nearest neighbors lists of *highly recommended* according to BasicTRL and RF2 contain only pivots from the PosPiv class.

6 Conclusions

We proposed Task Refinement Learning algorithms for domain adaptation with representation learning. Our TRL algorithms are tailored to the PBLM representation learning model of ZR18 and aim to provide more effective training for this model. The resulting PBLM-CNN model improves both the accuracy and the stability of the original PBLM-CNN model where PBLM is trained without TRL.

In future work we would like to develop more sophisticated TRL algorithms, for both in-domain and domain adaptation NLP setups. Moreover, we would like to establish the theoretical groundings to the improved stability achieved by TRL, and to explore this effect beyond domain adaptation.

Acknowledgements

We would like to thank the members of the IE@Technion NLP group for their valuable feedback and advice. This research has been funded by an ISF personal grant on "Domain Adaptation in NLP: Combining Deep Learning with Domain and Task Knowledge".

References

Shai Ben-David, John Blitzer, Koby Crammer, Alex Kulesza, Fernando Pereira, and Jennifer Wortman Vaughan. 2010. A theory of learning from different domains. *Machine learning*, 79(1-2):151–175.

Yoshua Bengio, Jérôme Louradour, Ronan Collobert, and Jason Weston. 2009. Curriculum learning. In *Proceedings of the 26th annual international conference on machine learning*, pages 41–48. ACM.

John Blitzer, Mark Dredze, Fernando Pereira, et al. 2007. Biographies, bollywood, boom-boxes and blenders: Domain adaptation for sentiment classification. In *Proc. of ACL*.

John Blitzer, Ryan McDonald, and Fernando Pereira. 2006. Domain adaptation with structural correspondence learning. In *Proc. of EMNLP*.

Danushka Bollegala, Takanori Maehara, and Ken-ichi Kawarabayashi. 2015. Unsupervised cross-domain word representation learning. In *Proc. of ACL*.

Danushka Bollegala, Yutaka Matsuo, and Mitsuru Ishizuka. 2011. Relation adaptation: learning to extract novel relations with minimum supervision. In *Proc. of IJCAI*.

Ciprian Chelba and Alex Acero. 2004. Adaptation of maximum entropy capitalizer: Little data can help a lot. In *Proc. of EMNLP*.

Minmin Chen, Yixin Chen, and Kilian Q Weinberger. 2011. Automatic feature decomposition for single view co-training. In *Proc. of ICML*.

Minmin Chen, Zhixiang Xu, Kilian Weinberger, and Fei Sha. 2012. Marginalized denoising autoencoders for domain adaptation. In *Proc. of ICML*.

Stéphane Clinchant, Gabriela Csurka, and Boris Chidlovskii. 2016. A domain adaptation regularization for denoising autoencoders. In *Proc. of ACL (short papers)*.

Hal Daumé III. 2007. Frustratingly easy domain adaptation. In *Proc. of ACL*.

Hal Daumé III and Daniel Marcu. 2006. Domain adaptation for statistical classifiers. *Journal of Artificial Intelligence Research*, 26:101–126.

Jeffrey L Elman. 1993. Learning and development in neural networks: The importance of starting small. *Cognition*, 48(1):71–99.

Yaroslav Ganin, Evgeniya Ustinova, Hana Ajakan, Pascal Germain, Hugo Larochelle, François Laviolette, Mario Marchand, and Victor Lempitsky. 2016. Domain-adversarial training of neural networks. *Journal of Machine Learning Research*, 17(59):1–35.

Xavier Glorot, Antoine Bordes, and Yoshua Bengio. 2011. Domain adaptation for large-scale sentiment classification: A deep learning approach. In *In proc. of ICML*, pages 513–520.

Chen Gong, Dacheng Tao, Stephen J Maybank, Wei Liu, Guoliang Kang, and Jie Yang. 2016. Multi-modal curriculum learning for semi-supervised image classification. *IEEE Transactions on Image Processing*, 25(7):3249–3260.

Stephan Gouws, GJ Van Rooyen, MIH Medialab, and Yoshua Bengio. 2012. Learning structural correspondences across different linguistic domains with synchronous neural language models. In *Proc. of the xLite Workshop on Cross-Lingual Technologies, NIPS*.

Sepp Hochreiter and Jürgen Schmidhuber. 1997. Long short-term memory. *Neural computation*, 9(8):1735–1780.

Jiayuan Huang, Arthur Gretton, Karsten M Borgwardt, Bernhard Schölkopf, and Alex J Smola. 2007. Correcting sample selection bias by unlabeled data. In *Proc. of NIPS*.

Frank Hutter, Holger Hoos, and Kevin Leyton-Brown. 2014. An efficient approach for assessing hyperparameter importance. In *Proc. of ICML*.

Jing Jiang and ChengXiang Zhai. 2007. Instance weighting for domain adaptation in nlp. In *Proc. of ACL*.

Diederik Kingma and Jimmy Ba. 2015. Adam: A method for stochastic optimization. In *Proc. of ICLR*.

Diederik P Kingma and Max Welling. 2014. Auto-encoding variational bayes. In *Proc. of ICLR*.

Christos Louizos, Kevin Swersky, Yujia Li, Max Welling, and Richard Zemel. 2016. The variational fair autoencoder.

Yishay Mansour, Mehryar Mohri, and Afshin Rostamizadeh. 2009. Domain adaptation with multiple sources. In *Proc. of NIPS*.

David McClosky, Eugene Charniak, and Mark Johnson. 2010. Automatic domain adaptation for parsing. In *Proc. of NAACL*.

Quang Nguyen. 2015. The airline review dataset. `https://github.com/quankiquanki/skytrax-reviews-dataset`. Scraped from `www.airlinequality.com`.

Junhyuk Oh, Xiaoxiao Guo, Honglak Lee, Richard L Lewis, and Satinder Singh. 2015. Action-conditional video prediction using deep networks in atari games. In *Proc. of NIPS*.

Sinno Jialin Pan, Xiaochuan Ni, Jian-Tao Sun, Qiang Yang, and Zheng Chen. 2010. Cross-domain sentiment classification via spectral feature alignment. In *Proceedings of the 19th international conference on World wide web*, pages 751–760. ACM.

Anastasia Pentina, Viktoriia Sharmanska, and Christoph H Lampert. 2015. Curriculum learning of multiple tasks. In *Proc. of CVPR*, pages 5492–5500.

Nils Reimers and Iryna Gurevych. 2017. Reporting score distributions makes a difference: Performance study of lstm-networks for sequence tagging. In *Proc. of EMNLP*.

Danilo Jimenez Rezende, Shakir Mohamed, and Daan Wierstra. 2014. Stochastic backpropagation and approximate inference in deep generative models. In *Proc. of ICML*.

Brian Roark and Michiel Bacchiani. 2003. Supervised and unsupervised pcfg adaptation to novel domains. In *Proc. of HLT-NAACL*.

Alexander M Rush, Roi Reichart, Michael Collins, and Amir Globerson. 2012. Improved parsing and pos tagging using inter-sentence consistency constraints. In *Proc. of EMNLP-CoNLL*.

Mrinmaya Sachan and Eric Xing. 2016. Easy questions first? a case study on curriculum learning for question answering. In *Proc. of ACL*.

Tobias Schnabel and Hinrich Schütze. 2014. Flors: Fast and simple domain adaptation for part-of-speech tagging. *Transactions of the Association for Computational Linguistics*, 2:15–26.

Yangyang Shi, Martha Larson, and Catholijn M Jonker. 2015. Recurrent neural network language model adaptation with curriculum learning. *Computer Speech & Language*, 33(1):136–154.

Valentin I Spitkovsky, Hiyan Alshawi, and Daniel Jurafsky. 2010. From baby steps to leapfrog: How less is more in unsupervised dependency parsing. In *Proc. of NAACL-HLT*.

Ivan Titov. 2011. Domain adaptation by constraining inter-domain variability of latent feature representation. In *Proc. of ACL*.

Joseph Turian, Lev Ratinov, and Yoshua Bengio. 2010. Word representations: a simple and general method for semi-supervised learning. In *Proc. of ACL*.

Pascal Vincent, Hugo Larochelle, Yoshua Bengio, and Pierre-Antoine Manzagol. 2008. Extracting and composing robust features with denoising autoencoders. In *Proc. of ICML*.

John Wieting, Mohit Bansal, Kevin Gimpel, and Karen Livescu. 2016. Charagram: Embedding words and sentences via character n-grams. In *Proc. of EMNLP*.

Yi Yang and Jacob Eisenstein. 2014. Fast easy unsupervised domain adaptation with marginalized structured dropout. In *Proc. of ACL (short papers)*.

Jianfei Yu and Jing Jiang. 2016. Learning sentence embeddings with auxiliary tasks for cross-domain sentiment classification. In *Proc. of EMNLP*.

Yang Zhang, Philip David, and Boqing Gong. 2017. Curriculum domain adaptation for semantic segmentation of urban scenes. In *The IEEE International Conference on Computer Vision (ICCV)*, volume 2, page 6.

Yftah Ziser and Roi Reichart. 2017. Neural structural correspondence learning for domain adaptation. In *Proc. of CoNLL*.

Yftah Ziser and Roi Reichart. 2018a. Pivot based language modeling for improved neural domain adaptation. In *Proceedings of the 2018 Conference of the North American Chapter of the Association for Computational Linguistics: Human Language Technologies, Volume 1 (Long Papers)*, volume 1, pages 1241–1251.

Yftah Ziser and Roi Reichart. 2018b. Deep pivot-based modeling for cross-language cross-domain transfer with minimal guidance. In *Proceedings of the 2018 Conference on Empirical Methods in Natural Language Processing*, pages 238–249.

Will Y Zou, Richard Socher, Daniel Cer, and Christopher D Manning. 2013. Bilingual word embeddings for phrase-based machine translation. In *Proc. of EMNLP*.

A URLs of Code and Data

As noted in the experiments section, we provide here the URLs for the code and data we use in the paper.

- Blitzer et al. (2007) product review data: http://www.cs.jhu.edu/~mdredze/datasets/sentiment/index2.html.
- The airline review data is (Nguyen, 2015).
- Code for the PBLM and PBLM-CNN models (Ziser and Reichart, 2018a): https://github.com/yftah89/PBLM-Domain-Adaptation.
- Code for the AE-SCL and AE-SCL-SR models of ZR17 (Ziser and Reichart, 2017): https://github.com/yftah89/Neural-SCLDomain-Adaptation.
- Code for the SCL-MI method of Blitzer et al. (2007): see footnote [6] (the URL does not fit into the line width).
- Code for MSDA (Chen et al., 2012): http://www.cse.wustl.edu/~mchen.
- Code for the domain adversarial network used as part of the MSDA-DAN baseline (Ganin et al., 2016): https://github.com/GRAAL-Research/domain_adversarial_neural_network.
- Logistic regression code: http://scikit-learn.org/stable/.

B Hyperparameter Tuning

As noted in the experimental setup, for all previous work models (except from the PBLM models of (Ziser and Reichart, 2018a)), we follow the experimental setup of (Ziser and Reichart, 2017) including their hyperparameter estimation protocol. The hyperparameters of the PBLM models are provided here (they are identical to those of (Ziser and Reichart, 2018a)):

- Input word embedding size: $(128, 256)$.
- Number of pivot features: $(100, 200, 300, 400, 500)$.
- $|h_t| : (128, 256, 512)$.
- PBLM model order: second order.

Note that Ziser and Reichart (2018a) also considered the word embedding size of 32 and 64. In our preliminary experiments these hyperparameters provided very poor performance for the plain PBLM model, so we excluded them from our full set of experiments.

For the CNN in PBLM-CNN we only experimented with $K = 250$ filters and with a kernel of size $d = 3$.

All the algorithms in the paper that involve a LSTM or a CNN are trained with the ADAM algorithm (Kingma and Ba, 2015). For this algorithm we used the parameters described in the original ADAM article (these parameters were also used by ZR18):

- Learning rate: $lr = 0.001$.
- Exponential decay rate for the 1st moment estimates: $\beta_1 = 0.9$.
- Exponential decay rate for the 2nd moment estimates: $\beta_2 = 0.999$.
- Fuzz factor: $\epsilon = 1e - 08$.
- Learning rate decay over each update: $decay = 0.0$.

For all the experiments in the paper we use the same random seed for parameter initialization.

C Experimental Details

Pre-processing All sequential models considered in our experiments are fed with one review example at a time. For all models in the paper, punctuation is first removed from the text before it is processed by the model (sentence boundaries are still encoded). This is the only pre-processing step we employ in the paper. This decision is in line with Ziser and Reichart (2018a).

Features For AE-SCL-SR, SCL-MI and MSDA we concatenate the representation learned by the model with the original representation and this representation is fed to the logistic regression classifier. MSDA-DAN jointly learns the feature representation and performs the sentiment classification task. It is hence fed by a concatenation of the original and the MSDA-induced representations.

[6] https://github.com/yftah89/structural-correspondence-learning-SCL